Desalination and Water Treatment
www.deswater.com
doi: 10.5004/dwt.2018.22393

118 (2018) 181–194
June

Zinc and nickel removal from aqueous solution by activated carbon in batch and permeable reactive barrier (PRB) systems

M.A. Ale Ebrahim, T. Ebadi*

Civil Engineering Department, Amirkabir University, Tehran 15875-4413, Iran,
emails: m.aleebrahim@aut.ac.ir (M.A. Ale Ebrahim), tebadi@aut.ac.ir (T. Ebadi)

Received 29 July 2017; Accepted 21 April 2018

ABSTRACT

In this work, factors that affect removal of zinc ion from aqueous solution by activated carbon were evaluated using the response surface methodology. The effects of concentration, pH, and activated carbon/solution ratio on removal efficiency were considered, and optimum conditions were determined. Then, the kinetics and equilibrium equations were expressed. Maximum removal efficiency for zinc in batch tests reached 96.7%. Moreover, co-adsorption of zinc and nickel ions was studied. Zn removal efficiency when Ni ions were present was enhanced surprisingly. Also, single Zn, as well as a system containing Zn and Ni ions, removal in a permeable reactive barrier was investigated. Single zinc breakthrough time reached 60 h, while similar breakthrough in a system containing Zn and Ni ions reached 65 h. Finally, various regeneration tests were conducted with over 90% desorption efficiency.

Keywords: Zinc removal; Activated carbon; Response surface methodology; Co-adsorption of Zn and Ni ions; Permeable reactive barrier

1. Introduction

High-quality drinking water is one of the most important preliminary necessities for human life. Among different kinds of water pollutants, toxic heavy metal ions are the main problem. The most common heavy metals are cadmium, chromium, cobalt, copper, lead, mercury, nickel, and zinc [1]. Some of these ions could have possible benefits in allowable concentrations but create serious hazards if they overpass relative limit of concentration.

Zinc and nickel are of moderate toxicity and have widespread presence in various industries such as galvanization, metal finishing, ceramic, photographic paper, rubber vulcanization accumulator, textiles, and battery manufacturing [2]. Maximum acceptable limits of Zn and Ni from standards in potable water are 3.0 and 0.5 mg/L, respectively [2,3].

Currently, the most common processes for heavy metal elimination are adsorption, reverse osmosis, ion exchange, coagulation, membrane filtration, and chemical precipitation [4]. In fact, adsorption with a suitable adsorbent, such as activated carbon, is a conventional method due to low fixed costs.

Although various adsorbents made by different materials such as rice husk [5], rubber tires [6], bagasse [7], and walnut shell [8] were investigated to remove Zn and Ni from water, high surface area commercial coal-based activated carbon is still the most widely used adsorbent [9]. Moreover, it is possible to convert some agricultural wastes (such as pistachio shell) to activated carbon simply, which can be relatively similar to chosen adsorbent in the present work but with applying the principles of green chemistry.

Generally, activated carbons can be prepared via a physical or a chemical method. The physical method involves two pyrolysis and physical activation stages. In the first pyrolysis stage, the starting material is carbonized in an inert atmosphere at moderate temperatures to produce char. Subsequently, in the second activation stage, the resulting char is subjected to a partial gasification reaction at higher temperatures with steam or carbon dioxide to produce final activated carbon. Physical activation by H_2O or CO_2 is more environment-friendly process than chemical activation by reagents such as $ZnCl_2$, KOH, and H_3PO_4 [10].

* Corresponding author.

There are numerous works about adsorption of heavy metals by activated carbon in the literature. For example, iron adsorption performance has been compared on biosorbent, biochar, and activated carbon [11]. The influence of modification of activated carbon has been reported on cadmium removal [12]. A comparative study of lead removal by activated carbon, kaolin, bentonite, blast furnace slag, and fly ash has been performed [13]. Effect of impregnation of activated carbon by humic acid on mercury removal efficiency has been considered [14]. On the other hand, manganese adsorption by activated carbon has been studied by an experimental design method [15]. Finally, an acid-modified activated carbon has been used for toxic chromium(VI) ion removal [16].

In terms of zinc adsorption by various activated carbons, some studies examined using *Bambusa vulgaris striata* [17], coconut shell source [18], and modified coal-based source [19]. On the other hand, nickel adsorption has been considered by cyclopolymer adsorbent [20], polystyrene-based [21], pine-needle-based [22], and olive-stone-based [23] activated carbons.

However, a very few studies examined co-adsorption of metal ions by activated carbon. For example, competitive Cu and Pb adsorption from aqueous solution on activated carbon was examined [24]. Moreover, simultaneous adsorption of Zn and Ni ions on activated carbon fibers has been investigated [25].

Permeable reactive barriers (PRBs) have been proposed for groundwater treatment [26]. Some applications of PRBs are Cr removal [27], acid mine remediation [28], Se immobilization [29], hydrocarbon contaminated groundwater treatment [30], and zinc removal from water by a rock barrier [31]. Moreover, some aspects of design, experimental procedure, and efficiency of PRBs have been reported in the literature. For example, eight metals removal from acid mine drainage was performed by limestone and red mud PRB [32]. Also, modeling of reaction front progress in multi-component metals removal by fly ash PRB was accomplished [33]. On the other hand, the fate of contaminants by zero-valent iron was investigated [34]. The geochemical modeling of waste iron and sand mixture PRB was also studied [35]. Finally, removal of some heavy metals was performed by organic/inorganic PRB system [36].

In this work, the removal of single Zn ion in aqueous solution by activated carbon was accomplished using response surface methodology (RSM) experimental design. The removal efficiency was expressed as a function of operating conditions consisted of zinc concentration, pH, and carbon/water ratio, and optimum conditions were estimated, as well. Moreover, equations for kinetics and equilibrium (thermodynamics) of single-ion zinc solution were presented. Then, co-adsorption of zinc and nickel ions of water, by activated carbon, was studied batch-wise. Finally, a PRB system was constructed for continuous metal removal from an aqueous stream by activated carbon. The performances of PRB for single Zn, and a Zn and Ni mixture removal in long-time tests were determined. Also, regeneration of spent adsorbents was performed by acid desorption. Hence, an innovative aspect of this work is to perform a comprehensive study on zinc adsorption by activated carbon including kinetics, equilibrium, thermodynamics, RSM optimization of effective adsorption parameters, co-adsorption of zinc and nickel, PRB continuous tests, and regeneration of spent adsorbent.

2. Materials and methods

2.1. Raw materials

The activated carbon used in this study was purchased from Jacobi (a Sweden company), type AquaSorb 2000. This type is 8–30 mesh (0.6–2.36 mm) granular coal-based activated carbon for wide range of water treatment application. The reported iodine number of this activated carbon is 950 mg/g, and total ash content is 13%. Brunauer–Emmett–Teller (BET) surface area, Saito and Foley method micro-pore volume, and Barrett–Joyner–Halenda method meso-pore volume of this activated carbon were determined (by Autosorb 1-MP from Quantachrome in this work) as 1,064 m^2/g, 0.50 mL/g and 1.36 mL/g, respectively.

A high purity casting grade sand (97.5% SiO_2) with 0.5–0.9 mm diameter was used in PRB compartments.

Zinc and nickel solutions were prepared from pure $Zn(NO_3)_2.6H_2O$ and $Ni(NO_3)_2.6H_2O$ (from ChemLab, Belgium) dissolution in distilled water.

2.2. Experimental methodology

2.2.1. Adsorption experimental procedures

All adsorption experiments were carried out batch-wise in a 400-mL glass vessel (100 mL liquid volume) with adequate magnetic stirring. The pH value was controlled (between 2 and 6) by dilute nitric acid solution and monitored by a digital pH meter. The chosen zinc ion concentration for experimental design was between 20 and 60 mg/L, and activated carbon content was between 0.5 and 2.5 g/100 mL of solution. The conditions for zinc ion in kinetic and equilibrium tests were pH = 6, 50 mg/L initial concentration, and adsorbent concentration: 2.5 g of activated carbon in 100 mL solution. The sampling times for kinetic test were 15 min up to 90 min, and then, 30 min up to 240 min. Finally, the conditions for co-adsorption of Zn and Ni ions in batch tests were pH 6, adsorbent concentration: 2.5 g of activated carbon in 100 mL solution, and initial metal ion concentration ratios (mg/L) 40/40, 40/60, and 60/40. At different times after contacting of activated carbon granules and Zn or Zn and Ni solution, sampling was performed by a small (1 mL) pipette.

2.2.2. Kinetic studies

The metal removal is defined as Eq. (1):

$$\text{Metal removal (\%)} = \frac{(C_0 - C_e)}{C_0} \times 100 \quad (1)$$

where C_0 is the initial metal concentration (mg/L), and C_e is the final concentration of the metal (mg/L).

Pseudo-first-order, pseudo-second-order, intra-particle diffusion, and Elovich kinetic equations are described briefly in Table 1 [37]. The pseudo-first-order kinetics assumes that rate of adsorption is proportional to the number of unoccupied sites of activated carbon. On the other hand, rate of adsorption in the pseudo-second-order equation is proportional to the square number of unoccupied sites of the activated carbon. The intra-particle diffusion assumes that the solute uptake varies almost proportionally with square root

of time. Finally, Elovich kinetic model considers solid surface as an energetically heterogeneous structure [38].

2.2.3. Equilibrium studies

The equilibrium study of zinc ion removal by activated carbon was performed at pH = 6, adsorbent concentration: 1.5 g of activated carbon in 100 mL solution, 3 h mixing time, and 30, 45, 60, and 80 mg/L initial concentrations. Various equilibrium models consisting of Langmuir, Freundlich, Dubinin–Radushkevich (D–R), and Temkin equations are briefly described in Table 2 [38]. The assumption for Langmuir model is equivalent sorption of activation energies. On the other hand, Freundlich equation assumes logarithmic

Table 1
Various kinetic equations for adsorption

Model	Equation	Plot
Pseudo-first-order kinetic	$\mathrm{Log}(q_e - q_t) = \mathrm{Log}(q_e) - \frac{K_1}{2.303}t$	$\mathrm{Log}(q_e - q_t)$ vs. t
Pseudo-second-order kinetic	$\frac{t}{q_t} = \frac{1}{K_2 q_e^2} + \frac{t}{q_e}$	$\frac{t}{q_t}$ vs. t
Intra-particle diffusion	$q_t = K_{\mathrm{int}} t^{0.5} + C$	q_t vs. $t^{0.5}$
Elovich	$q_t = \frac{1}{\beta}\mathrm{Ln}(\alpha\beta) + \frac{1}{\beta}\mathrm{Ln}(t)$	q_t vs. $\mathrm{Ln}(t)$

Note: q_e: adsorption capacities at equilibrium (mg/g), q_t: adsorption capacities at time t (mg/g), K_1: rate constant of pseudo-first-order adsorption (1/min), K_2: rate constant of pseudo-second-order adsorption (g/mg min), K_{int}: intra-particle diffusion rate constant (mg/g $\mathrm{min}^{0.5}$), C: y-intercept of intra-particle diffusion plot (mg/g), α: initial rate (mg/g min), and β: Elovich constant (g/mg).

Table 2
Various equilibrium equations for adsorption

Model	Equation	Plot
Langmuir isotherm	$\frac{C_e}{q_e} = \frac{1}{q_m b} + \frac{C_e}{q_m}$	$\frac{C_e}{q_e}$ vs. C_e
Freundlich isotherm	$q_e = K_f C_e^{\frac{1}{n}}$ or $\mathrm{Ln}(q_e) = \mathrm{Ln}(K_f) + \frac{1}{n}\mathrm{Ln}(C_e)$	$\mathrm{Ln}(q_e)$ vs. $\mathrm{Ln}(C_e)$
Dubinin–Radushkevich (D–R) isotherm	$q_e = q_s \exp(-K_D \varepsilon^2)$ or $\mathrm{Ln}(q_e) = \mathrm{Ln}(q_s) - K_D R^2 T^2 \left[\mathrm{Ln}\left(1 + \frac{1}{C_e}\right)\right]^2$ $E_s = \frac{1}{(2K_D)^{0.5}}$ $\varepsilon = RT\,\mathrm{Ln}\left(1 + \frac{1}{C_e}\right)$	$\mathrm{Ln}(q_e)$ vs. $\left[\mathrm{Ln}\left(1 + \frac{1}{C_e}\right)\right]^2$
Temkin isotherm	$q_e = \frac{RT}{B}\mathrm{Ln}(AC_e)$ $q_e = \frac{RT}{B}\mathrm{Ln}(A) + \frac{RT}{B}\mathrm{Ln}(C_e)$	q_e vs. $\mathrm{Ln}(C_e)$

Note: q_m: maximum adsorption capacity (mg/g), b: Langmuir constant (L/mg), K_f: Freundlich constant (mg/g), n: adsorption intensity, K_D: D–R constant related to mean free energy of adsorption ($\mathrm{mol}^2/\mathrm{kJ}^2$), R: universal gas constant (8.314 J/mol K), q_s: theoretical saturation capacity (mg/g), ε: Polanyi potential (kJ/mol), E_s: mean free energy of biosorption (kJ/mol), T: temperature (K), B: equilibrium binding constant (J/mol), and A: Temkin isotherm constant (L/mg).

decrease of activation energy with respect to surface coverage. Temkin model assumption is linear decrease in heat of adsorption versus surface coverage. Finally, D–R equation considers the characterization of sorption curve as a function of solid porous structure [38].

The amount of adsorbed metal per gram of carbon at equilibrium is determined by Eq. (2):

$$q_e = \frac{(C_0 - C_e)V}{m} \tag{2}$$

where q_e is amount of adsorbed metal per gram of adsorbent at equilibrium (mg/g), C_0 and C_e are concentrations of the metal ions before and after adsorption, respectively (mg/L), V is volume of the aqueous phase (L), and m is the mass of adsorbent (g).

2.2.4. Thermodynamic studies

Finally, in thermodynamics, van 't Hoff plot was considered from various adsorption tests at different temperatures. Then, this plot is used for the estimation of adsorption parameters from Eq. (3) [39]:

$$\Delta G^\circ = -RT\,\mathrm{Ln}(K_c) = -RT\,\mathrm{Ln}\left(\frac{mq_e}{VC_e}\right) \rightarrow \mathrm{Ln}(K_c) = -\frac{\Delta H^\circ}{RT} + \frac{\Delta S^\circ}{R} \tag{3}$$

where ΔG° standard free energy; K_c is equilibrium constant; and ΔH° and ΔS° are enthalpy and entropy of adsorption, respectively. Thus, by plotting Ln (Kc) vs. inverse of temperature, enthalpy and entropy of adsorption are determined.

2.2.5. Experimental design theory

Experimental design can be used for evaluation of the effects of operating parameters on the metal ion removal from aqueous solution by activated carbon. RSM is a powerful method for analyzing the influences of operating conditions on dependent variable or response. This method postulates a functional correlation between objective function and independent variables. The second-order RSM model can be presented by Eq. (4) [40]:

$$y = \beta_0 + \beta_1 A + \beta_2 B + \beta_3 C + \beta_{11} A^2 + \beta_{22} B^2 + \beta_{33} C^2 + \beta_{12} AB + \beta_{13} AC + \beta_{23} BC \tag{4}$$

where y is the process response (dependent variable); β_0 is constant, β_1, β_2, and β_3 are linear coefficients; β_{12}, β_{23}, and β_{13} are cross product coefficients; β_{11}, β_{22}, and β_{33} are quadratic coefficients; and A, B, and C are coded independent variables containing mass/100 mL (A), pH (B), and initial metal ion concentration (C) that are represented in terms of coded factors (–1, 0, and +1). A positive sign in the equation indicates a synergistic effect of the variables, while a negative sign represents an adverse effect of the variables [15].

2.2.6. Instrumental analysis

Analysis of single zinc or single nickel solutions was carried out by flame atomic absorption (AA) of Varian (240) with a good accuracy. However, AA results were poor in mixed metal system due to interference effect. Thus, for mixed Zn and Ni solutions, inductively coupled plasma (ICP) of Varian (Vista-PRO) was used.

2.2.7. PRB system

For the purpose of this study, a horizontal PRB was constructed from a thick glass (10 mm). Width, height, and total length of PRB were 13.5, 15, and 74 cm, respectively. A diagram of constructed PRB is presented in Fig. 1. The inlet polluted water was fed to the PRB by a burette with Q_f = 2.2 mL/min.

The PRB consisted of an initial polluted water compartment (5 cm), followed by a sand chest (10 cm), to maintain adequate water height and further horizontal flow, and a third polluted water chest (3 cm) before the activated carbon layer. Between the adjacent compartments, perforated Plexiglas sheets with 200 mesh steel laces were inserted. Then, in the fourth compartment (2.5 cm), a mixture of activated carbon and sand (1/2 weight ratio) was used as an adsorbent. After this layer, treated water (2.5 cm) and sand (40 cm) compartments exist. Finally, horizontal outlet flow of treated water emanates from the last water chest (10 cm).

The selected conditions in PRB tests were pH 6 and initial ion concentration ratio for Zn and Ni (mg/L) 60/30. Moreover, the permeability of sand in this PRB was estimated 0.04 cm/s, which is in the usual range of soil.

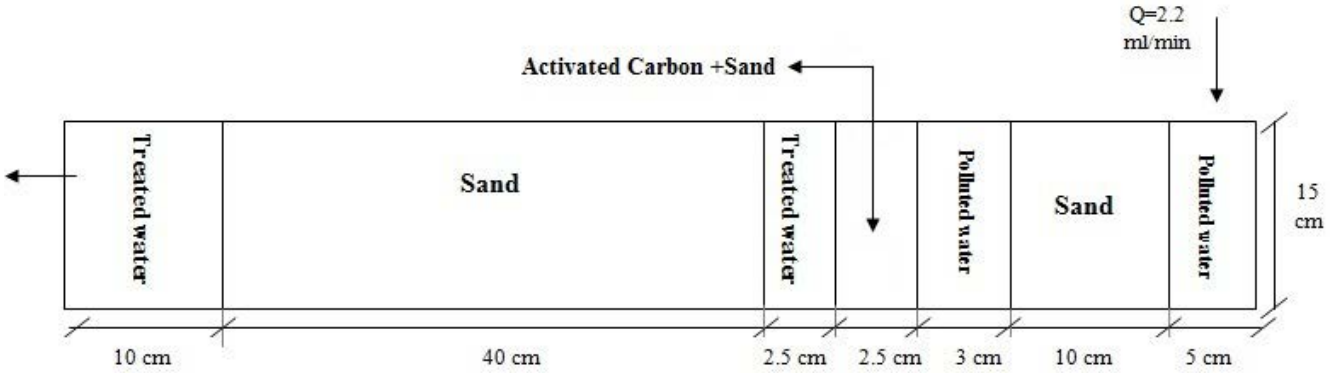

Fig. 1. Diagram of constructed PRB.

The prediction of asymptotic time of PRB for metal removal from an aqueous stream can be performed by Eq. (5) from equilibrium:

$$t_{\text{asym}} = \frac{1{,}000 q_m . m_c}{Q_f . C_f} \tag{5}$$

where C_f is concentration of metal in the PRB feed (mg/L); m_c is mass of carbon in PRB (g); Q_f is feed flow rate in PRB (L/min); and t_{asym} is asymptotic time of PRB for metal removal (min).

2.2.8. Regeneration

Desorption efficiency can be computed by Eq. (6) [41]:

$$D(\%) = \frac{C_d V_d}{(C_0 - C_e)V} \times 100 \tag{6}$$

where C_d is metal ion concentration in desorption solution (mg/L), and V_d is volume of desorption solution (L).

2.2.9. Activated carbon characterization

Characterizations of initial and modified activated carbons were done using BET surface area and pore size distribution tests by Autosorb 1-MP from Quantachrome.

Moreover, scanning electron microscope (SEM) photographs (Philips, XL-30) were taken from initial, spent, and regenerated activated carbon granules.

3. Results and discussion

3.1. Zinc removal kinetics and equilibrium

SEM pictures of initial, spent, and regenerated activated carbons are presented in Fig. 2. From this figure, macro-pores of a carbon granule can be easily seen. Moreover, bright metal points have been appeared in the carbon structure after adsorption. Finally, these metal points were almost disappeared after the regeneration.

Zn removal for the kinetic study tests versus time is presented in Fig. 3. Fig. 3 shows that 3 h agitation time is adequate for the experimental design and equilibrium tests.

The kinetic plots for Zn removal are illustrated in Fig. 4. The kinetic constants and correlation coefficients for Zn removal from the above-mentioned plots are reported in Table 3. As this table shows, the best kinetic model for zinc removal is pseudo-second-order equation. Consequently, Zn removal from aqueous solution by activated carbon is performed through a chemisorption phenomenon.

The results of plotting equilibrium equations are presented in Fig. 5 and Table 4. As Fig. 5 shows, Temkin (R^2 = 0.9947) and Langmuir (R^2 = 0.9924) equations are the best for zinc removal equilibrium. Dimensionless factor of separation in Langmuir model is defined by Eq. (7):

$$R_L = \frac{1}{1 + bC_0'} \tag{7}$$

where C_0' is the highest initial metal concentration. This parameter indicates that adsorption is unfavorable if $R_L > 1$, linear if $R_L = 1$, irreversible if $R_L = 0$, and favorable if $0 < R_L < 1$ [38]. Since R_L in Table 4 for zinc removal is 0.12, the adsorption of Zn is favorable.

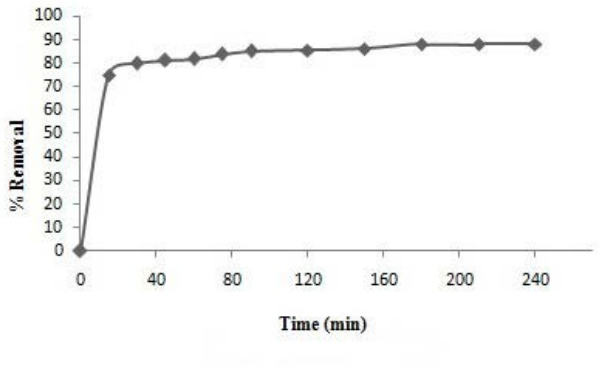

Fig. 3. The Zn removals versus time at 50 mg/L, pH = 6, and 2.5 g carbon/100 mL.

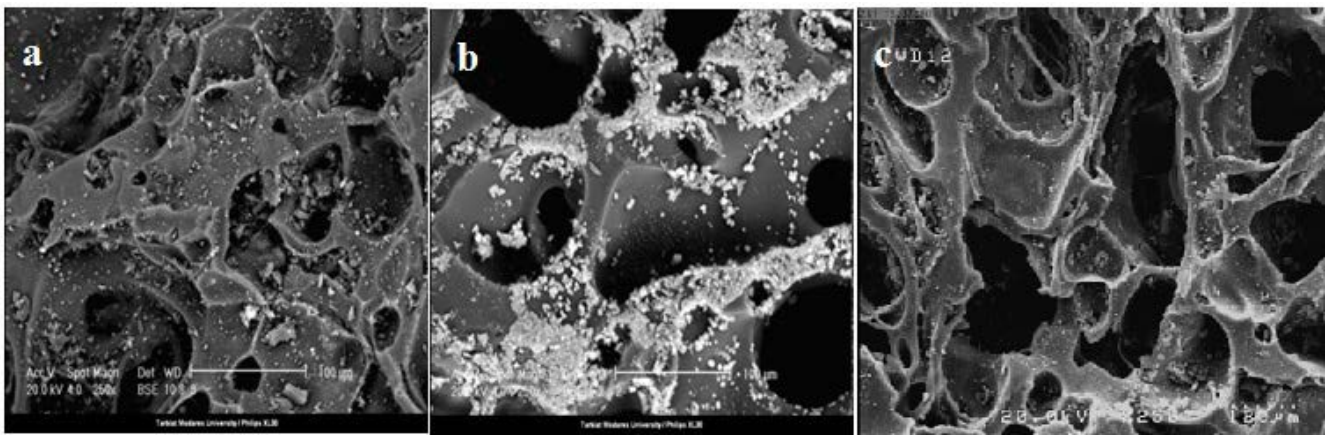

Fig. 2. SEM graphs (magnification: 250×) of initial activated carbon (a), activated carbon after zinc adsorption (b), and regenerated activated carbon (c).

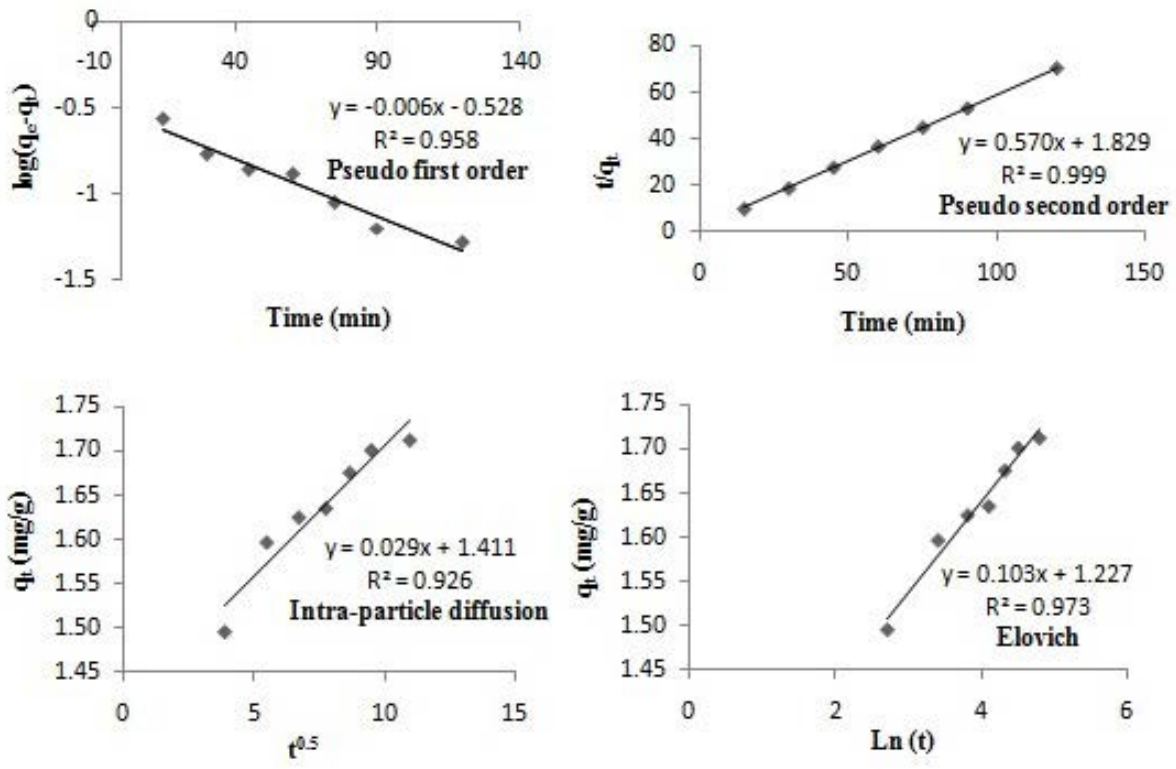

Fig. 4. The kinetic plots for Zn removal.

Table 3
The kinetic constants for Zn removal

Pseudo-first–order kinetics	K_1 (1/min)	0.014
	R^2	0.958
Pseudo-second–order kinetics	K_2 (g/mg min)	0.178
	R^2	0.999
Intra-particle diffusion	C	1.411
	K_{int} (mg/g min$^{0.5}$)	0.029
	R^2	0.926
Elovich	β (g/mg)	9.709
	α (mg/g min)	15,361.1
	R^2	0.973

In Freundlich isotherm, the value of parameter n determines the ability of adsorption. It is generally accepted that values of n in a range between 2 and 10 present good, 1 and 2 moderately difficult, and <1 indicate poor adsorption [38]. Since n (for zinc removal) in Table 4 is 1.77, the adsorption of Zn is moderately difficult. Moreover, q_m = 6.53 mg/g (Table 4) is found as maximum adsorption capacity of zinc on activated carbon in this work. This value is in close agreement with the reported q_m = 6.08 mg/g of an activated carbon produced from walnut shell for Zn removal [42].

Thermodynamic parameters of the tests at 28°C, 45°C, and 52°C were presented in Table 5. Since standard free energies are negative in Table 5, so adsorption process is feasible and thermodynamically favored [39]. Also, enthalpy values are positive indicating endothermic process, and entropy values are positive indicating affinity of carbon for zinc adsorption [39].

3.2. Zinc removal–RSM study

In this work, Box–Behnken RSM method was used (Design Expert, version 7.0.0). The effective parameters are pH, activated carbon/solution ratio, and the initial ion concentration. Moreover, each operating parameter is considered in three various levels. The experimental design operating conditions for Zn removal are illustrated in Table 6.

The RSM responses as zinc removal efficiency are presented in Table 7. In this table, twelve trials and five center points exist. ANOVA analysis and brief statistical study of zinc removal are shown in Tables 8 and 9.

The final predicting equation for zinc removal in the coded units (A, B, and C) is presented by Eq. (8):

$$y = 72.74 + 7.05A + 27.67B + 9.06C + \\ -0.87A^2 - 18.24B^2 - 7.63C^2 + 2.01AB + 4.09AC + 2.21BC \quad (8)$$

The significance of RSM method can be verified by high value of F and low value of p (<0.05) in ANOVA analysis. For zinc removal, this ANOVA table indicates the F-value of model equal to 50.55, which means that only 0.01% chance of "Model F-value" could be due to noise. Furthermore, the most objective function variation is due to regression

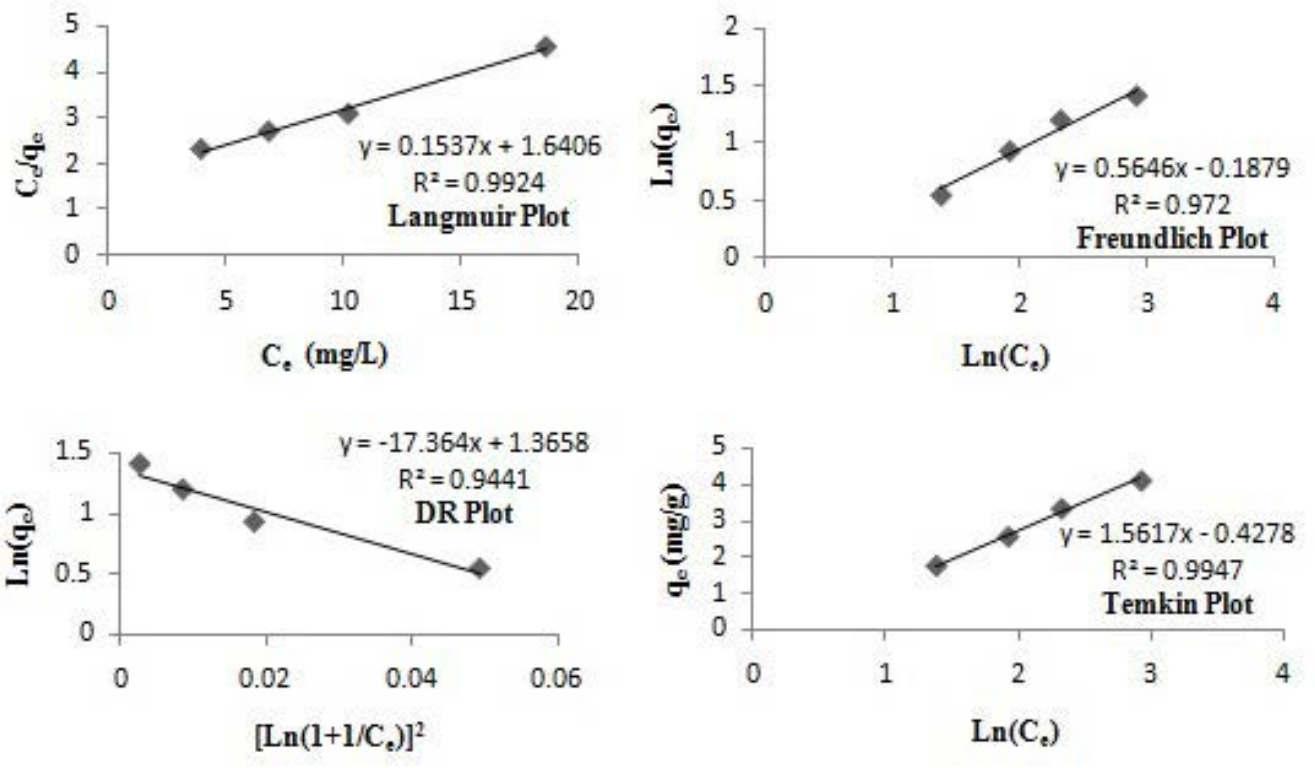

Fig. 5. Equilibrium plots for Zn removal.

Table 4
The equilibrium constants for Zn removal

Langmuir constants	q_m (mg/g)	6.53
	b (L/mg)	0.093
	R_L	0.12
	R^2	0.992
Freundlich constants	K_f (mg/g)	0.829
	n	1.773
	R^2	0.972
D–R constants	q_m (mg/g)	3.916
	K_D (mol²/kJ²)	2.925
	E_s (kJ/mol)	0.413
	R^2	0.944
Temkin constants	B (J/mol)	1,561
	A (L/mg)	0.761
	R^2	0.994

Table 5
Estimation of enthalpy and entropy of adsorption

T (K)	$-\Delta G$ (kJ/mol)	ΔS (J/mol K)	ΔH (kJ/mol)
301	7.97		
313	9.39	218.24	58.12
326	13.46		

Table 6
The experimental design operating conditions for Zn removal

Factor	Variable	Low (–1)	Middle (0)	High (+1)
A	Carbon mass (g/100 cc)	0.5	1.5	2.5
B	pH	2	4	6
C	Concentration (mg/L)	20	40	60

correlation, and thus, the significance of the model is verified. Moreover, its slow probability ($p < 0.0001$) indicates that the correlation is significant. In this study, A, B, C, B^2 and C^2 are significant terms for zinc removal. Other terms in Table 8, whose values of p are higher than 0.1, are not significant.

Also, "Lack-of-Fit F-value" determines the failure of correlation to fit the experimental data. Small F-values (2.91), obtained for lack-of-fit, are found to be non-significant, and also, there is 16.47% chance that "Lack-of-Fit F-value" in the zinc removal adsorption model could be due to noise. Moreover, considering values, "Predicted R^2" (0.826) was relatively in agreement with the "Adjusted R^2" (0.965). Finally, "Adequacy Precision" indicates the ratio of signal to noise, and ratios higher than 4 are desirable. The ratio of 22.85, in this work, shows a high value of signal, and thus, the proposed model can be applied for design space navigation.

Maximum zinc removal from RSM scenarios was proposed as 98.39% at pH = 5.75, adsorbent concentration: 2.5 g of activated carbon in 100 mL solution, and 59.95 mg/L initial

Table 7
The RSM responses as zinc removal efficiency

Standard order	Run	*A*: Mass/100 cc (g)	*B*: pH	*C*: Concentration (mg/L)	Zn removal (%)	
					Actual value	Predicted value
1	2	0.5	2	40	23	19.69
2	1	2.5	2	40	29.5	29.41
3	6	0.5	6	40	73.75	71.75
4	4	2.5	6	40	88.3	89.55
5	15	0.5	4	20	47.5	52.16
6	16	2.5	4	20	57	57.92
7	3	0.5	4	60	63.3	59.76
8	12	2.5	4	60	89.16	81.25
9	11	1.5	2	20	15	12.02
10	13	1.5	6	20	66.5	63.32
11	5	1.5	2	60	22.83	22.82
12	7	1.5	6	60	83.16	83.72
13	14	1.5	4	40	72.05	71.71
14	9	1.5	4	40	70.12	71.71
15	10	1.5	4	40	76.1	71.71
16	8	1.5	4	40	69.18	71.71
17	17	1.5	4	40	76.25	71.71

Table 8
Analysis of ANOVA for zinc removal

Source	Sum of squares	DF[a]	Mean square	*F*-value[b]	*p*-value (prob > *F*)[c]	
Model	9,016.9	9	1,001.88	50.55	<0.0001[s]	Significant
A: Mass/100 cc	397.76	1	397.76	20.07	0.0029[s]	
B: pH	6,126.14	1	6,126.14	309.12	<0.0001[s]	
C: Concentration	656.13	1	656.13	33.11	0.0007[s]	
AB	16.20	1	16.20	0.82	0.3960[n]	
AC	66.91	1	66.91	3.38	0.1087[n]	
BC	19.49	1	19.49	0.98	0.3544[n]	
A^2	3.17	1	3.17	0.16	0.7012[n]	
B^2	1,400.06	1	1,400.06	70.65	<0.0001[s]	
C^2	245.28	1	245.28	12.38	0.0098[s]	
Residual	138.73	7	19.82			
Lack-of-fit	95.1	3	31.70	2.91	0.1647[n]	Not significant
Pure error	43.62	4	10.91			
Corrected total	9,155.63	16				

[a]Degrees of freedom.
[b]Test for comparing model with residual (error) variance.
[c]Probability of finding the observed *F* value when the null hypothesis is true.
[s]Significant at $p < 0.05$.
[n]Significant at $p > 0.05$.

Table 9
The brief statistical study for zinc removal

Standard deviation	4.45	R^2	0.985
Mean	60.16	Adjusted R^2	0.965
Coefficient of variation (%)	7.40	Predicted R^2	0.826
PRESS	1,589.79	Adequacy precision	22.85

concentration with 0.981 desirability. The zinc removal of the validation test for this condition was obtained as 96.7% with a good accuracy according to the prediction value. Thus, the remained zinc concentration after adsorption treatment is enough low.

Normal probability plot of residuals for Zn removal is shown in Fig. 6. Since the points are close to the related line in this figure, the model is validated. Moreover, a comparison between actual and predicted values is presented in Fig. 6, where a good performance can be seen. Finally, residuals versus predicted values are illustrated in Fig. 7. The model consistency is verified by high dispersion of the points in this figure.

Then, the effects of operating conditions were predicted by RSM. The effects of activated carbon/water ratio and pH of solution are presented in Fig. 8. Also, the effect of initial Zn concentration is illustrated in Fig. 9.

From Fig. 8, it is obvious that zinc removal is enhanced by increasing activated carbon/water ratio with a relatively low slope. Also, by increasing pH from 2 to about 5.5, the removal efficiency is increased sharply, and then, it is decreased up to pH = 6. Therefore, pH 5.7 is the best condition for zinc removal, which is in agreement with previous reported data [43].

Finally, Fig. 9 shows that between 20 and 50 mg/L, Zn removal efficiency is increased by a very low slope and then reached to a constant value between 50 and 60 mg/L. The experimental tests for equilibrium study are also presented in Fig. 9. Given that, in RSM design, there is no 30-mg/L test; forms of two curves in Fig. 9 are slightly different.

However, a decreasing trend of zinc removal efficiency after 25 mg/L (similar to experiments in Fig. 9) has been reported in literature [18]. The reason for increasing part of removal efficiency versus concentration has been attributed to zinc ion interaction to binding sites of solid [18]. While, decreasing part of removal efficiency versus concentration is due to saturation of adsorbent sites and consequently dominating ion exchange and pore diffusion mechanisms [18].

In addition, three-dimensional plots for binary interactions in zinc removal by activated carbon are presented in Fig. 10.

3.3. Co-adsorption of Zn and Ni ions in batch tests

Here, co-adsorption of Zn and Ni ions from aqueous solution by activated carbon in batch-wise tests is described. In actual waters or wastewaters, various metals exist simultaneously. Consequently, the effect of the first metal ion on adsorption behavior of the second metal can be studied in co-adsorption tests.

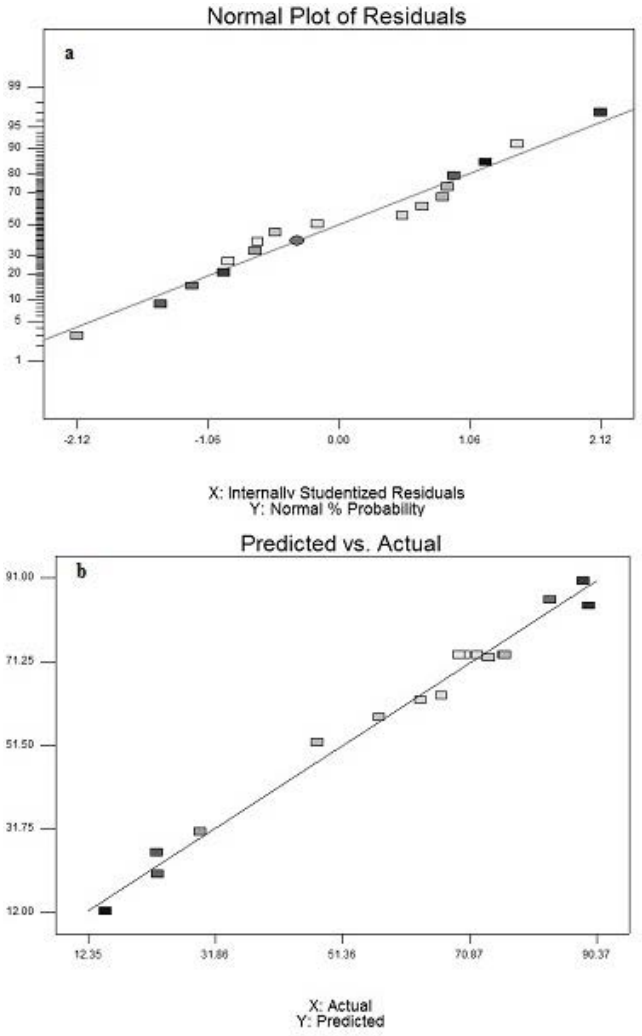

Fig. 6. The normal probability plot of residuals (a) and predicted values versus actual ones (b) for Zn removal in RSM.

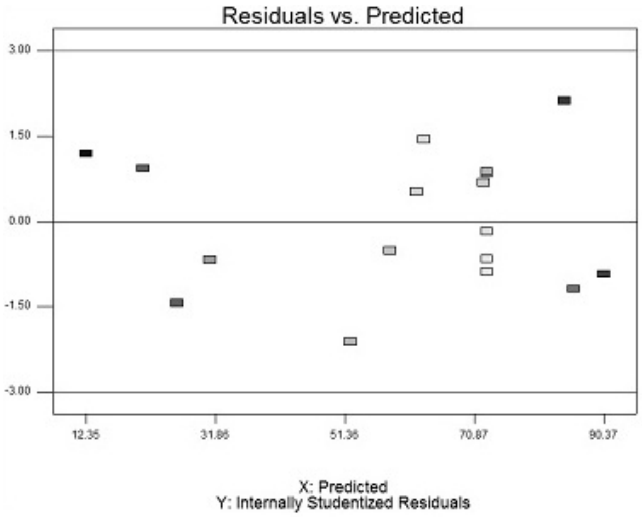

Fig. 7. The residuals versus predicted values for Zn removal in RSM.

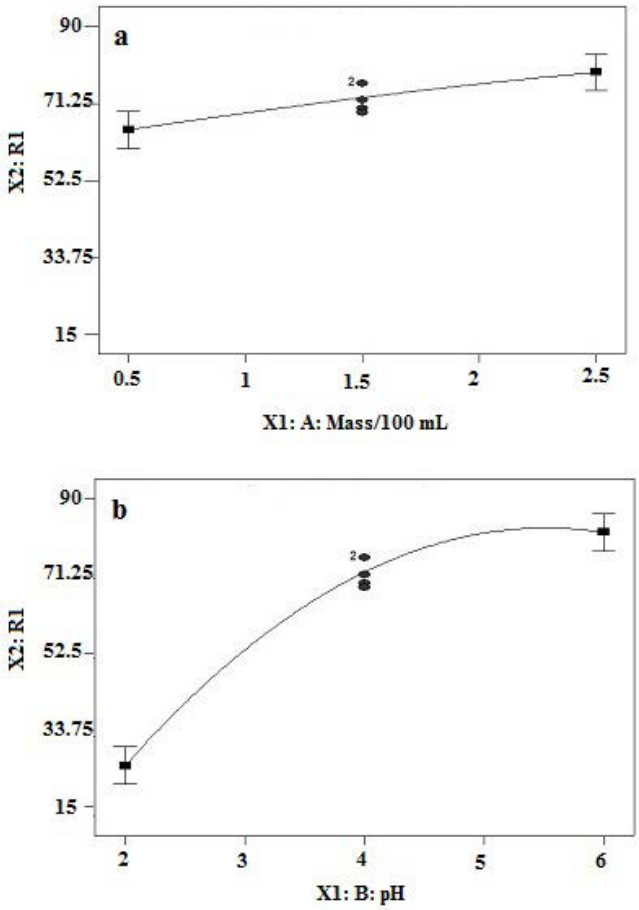

Fig. 8. Effect of carbon/water ratio (a) and pH (b) in Zn removal by RSM.

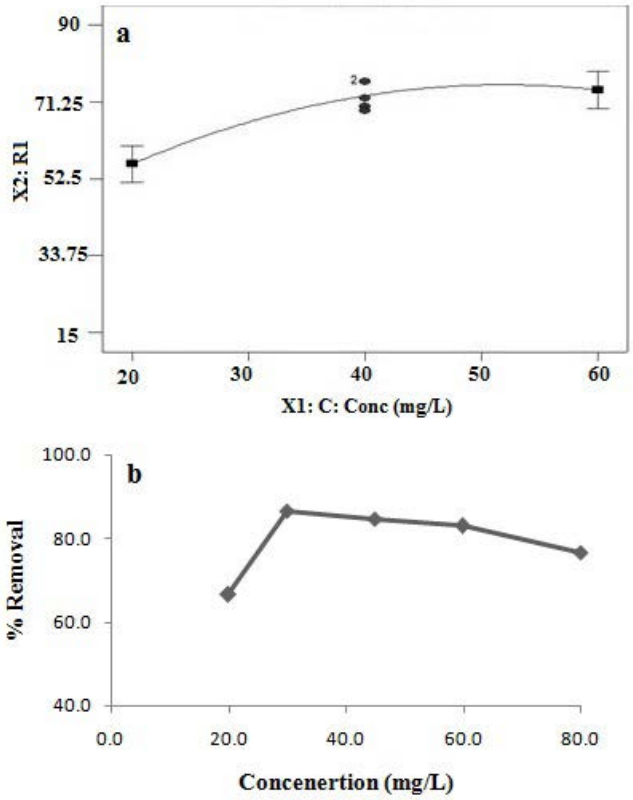

Fig. 9. Effect of concentration in Zn removal by RSM (a) and experimental results of equilibrium tests at pH = 6 and 1.5 g carbon/100 mL (b).

The accuracy of ICP results was verified by a standard mixture of 2.5 mg/L Zn and 2.5 mg/L Ni solution, in which ICP-determined concentrations were 2.11 mg/L Zn and 2.33 mg/L Ni.

The results for various single and mixed Zn and Ni ions adsorptions are presented in Table 10. As this table shows, the higher adsorption efficiency of single zinc (e.g., 88.3% at 40 mg/L) versus single nickel (67.8% at 40 mg/L) on activated carbon is obvious. This difference can be attributed to slightly higher ionic radius of zinc (0.74 Å) versus nickel (0.69 Å). A similar trend has been reported in the literature for lead (higher efficiencies for higher ionic radius) versus copper (lower ionic radius) adsorption [44].

Also, it is seen from Table 10 that the co-adsorption efficiency for Zn in the system containing also Ni ions was surprisingly enhanced compared with the system containing only Zn ions. The reason is probably the synergistic effect of the presence of Ni ions. The similar effect has been reported in co-adsorption of some binary mixtures such as Pb and Cu ions on biochar adsorbents [45,46].

However, nickel co-adsorption efficiency in mixed Zn and Ni system was diminished versus single Ni solution due to the usual competitive effect. This means most adsorption sites are occupied by one element (Zn), so there is not enough room for another metal ion (Ni) to be removed from the solution.

3.4. PRB tests for Zn, and Zn and Ni mixed streams

A PRB (or a permeable reactive treatment zone) is a cost-effective method for in situ groundwater treatment. For example, when groundwater is contaminated by a pollutant source, such as acid mine drainage or wastewater diffusion from soil, one usual technique is pumping and treatment. However, a relatively low-cost option consists of installation of permanent or even replaceable PRBs in the path of contaminant plumes [32]. Effective removal of some metals for long times (up to 45 d) has been reported for a PRB system [36]. Mathematical modeling of transport processes in PRB systems is based on advection-diffusion-reaction equations [33]. This means accumulation, convection through the bed, dispersion, and surface adsorption terms should be considered for simulation of a PRB system.

The PRB breakthrough data for a 60-mg/L zinc solution stream is presented in Fig. 11. As this figure shows, the lifetime for this test (single zinc solution) for PRB is about 60 h.

On the other hand, the PRB breakthrough data for Zn and Ni (60/30 mg/L) mixed solution stream is shown in Fig. 12. According to this figure, the related lifetime for PRB, in contact with zinc in the mixture, is about 65 h. This value

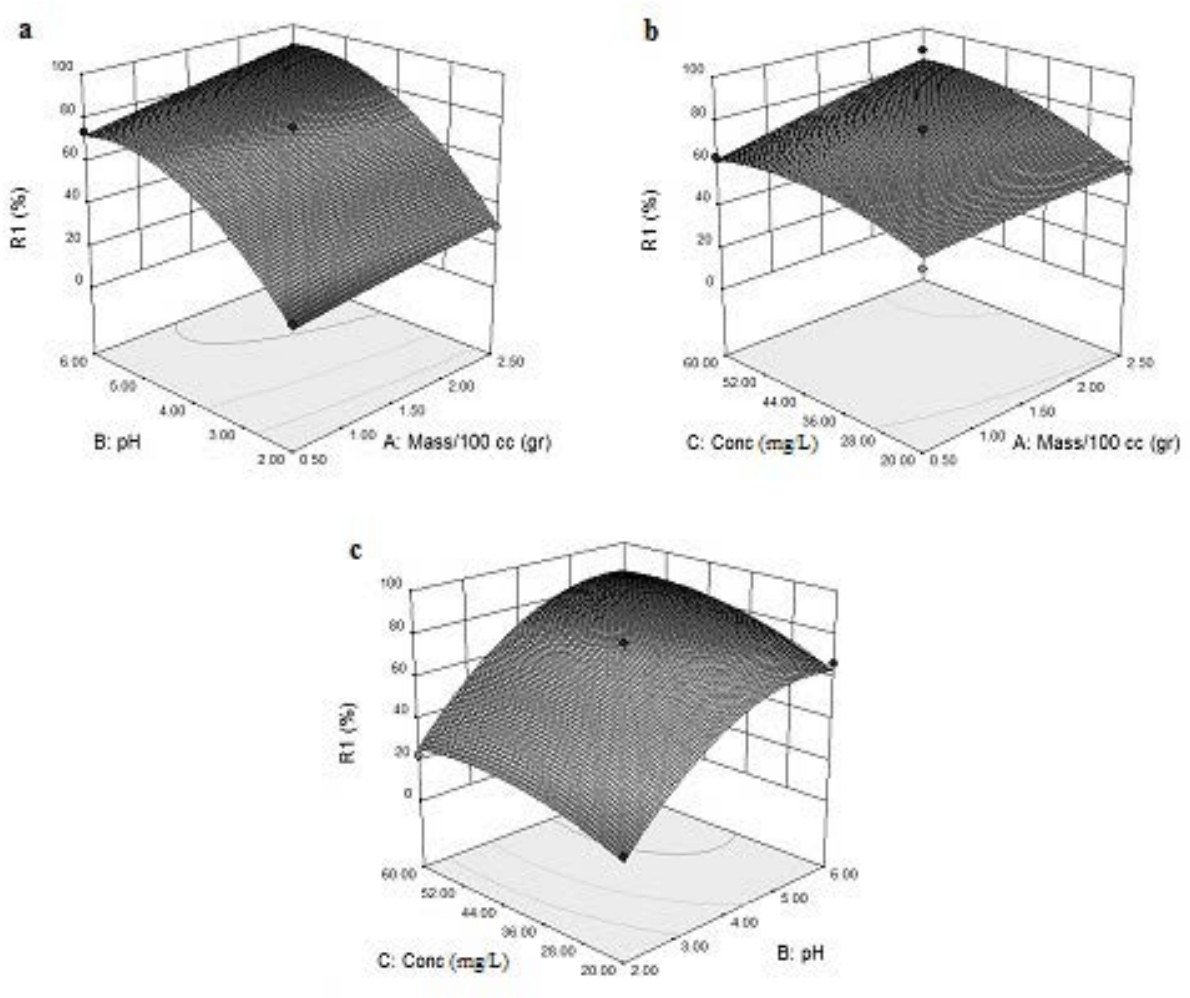

Fig. 10. Three-dimensional binary interaction plots for Zn removal in RSM.

Table 10
Results for various mixed Zn/Ni ions batch-wise solutions Zn removals

Zn/Ni initial concentrations ((mg/L) (mg/L))				Zn/Ni initial concentrations ((mg/L) (mg/L))			
Mass/100 cc	pH	Concentration	Ni removal %	Mass/100 cc	pH	Concentration	Zn removal %
2.5	6	40/40	48.25	2.5	6	40/40	95.75
2.5	6	60/40	44	2.5	6	60/40	93.16
2.5	6	40/60	41.16	2.5	6	40/60	95.75
2.5	6	0/40	67.75	2.5	6	40/0	88.3
2.5	6	0/60	61.67	2.5	6	60/0	85.52

is consistent with batch-wise previous results (enhanced Zn adsorption in the Zn and Ni mixtures ions).

The calculated value of asymptotic time for zinc removal tests from Eq. (5) is 113.8 h. This value is consistent with the experimental limiting case of Fig. 11. However, due to kinetic effect and finite residence times of polluted water stream in the adsorbent compartment of PRB, the actual lifetimes are much smaller than this.

The raw experimental PRB breakthrough curves (Figs. 11 and 12) can be used for the estimation of transport and adsorption parameters. For example, Peclet number (consisting of PRB dispersion coefficient) is evaluated based on curvature of the breakthrough curve. Moreover, some groundwater software programs such as STANDMOD, MODFLOW, and PHREEQC have been proposed for the estimation of such transport and adsorption parameters in the literature [47–49].

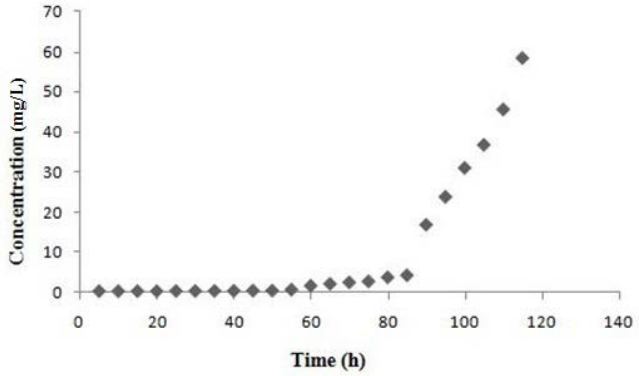

Fig. 11. PRB breakthrough curve data for zinc removal (feed concentration 60 mg/L).

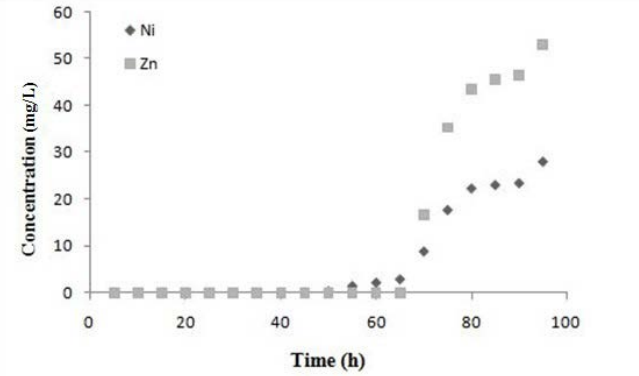

Fig. 12. PRB breakthrough curve data for Zn and Ni co-adsorption (60 mg/L Zn, and 30 mg/L Ni in feed).

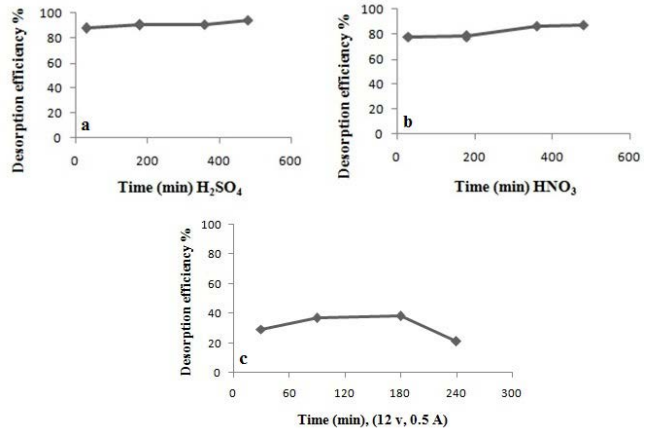

Fig. 13. Zinc desorption efficiencies versus time for 1 M sulfuric acid (a), 1 M nitric acid (b), and electrokinetic regeneration in water (c).

3.5. Regeneration of the spent adsorbents

Various regeneration experiments by H_2SO_4, HNO_3, and also electrokinetic tests (applying a low-level direct current to the spent adsorbent [16]) were performed in this work, and their efficiencies were compared with blank (distilled water) desorption test.

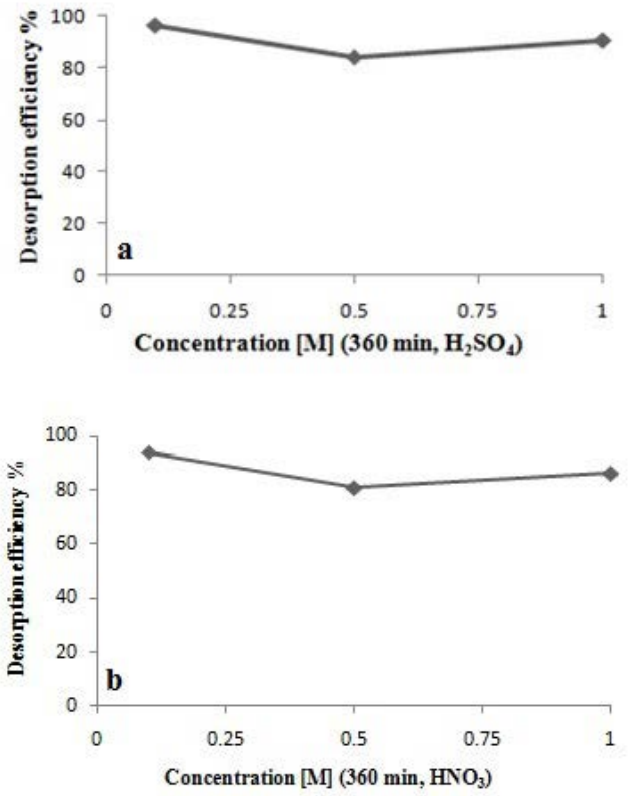

Fig. 14. Zinc desorption efficiencies after 6 h by various sulfuric acid concentrations (a) and various nitric acid concentrations (b).

The zinc desorption efficiency in distilled water after 6 h agitation was obtained about only 8%. Efficiency of the best electrokinetic test at 12 V, 0.5 A, and 3 h was determined as 20%.

On the other hand, zinc desorption by H_2SO_4 and HNO_3 were completely successful. In this field, an initial adsorption test was accomplished at the optimum condition. Then, the spent carbon was separated from solution and dried in an oven. Finally, desorption test was performed with the same carbon/acid solution ratio.

The results of sulfuric acid and nitric acid desorption at various times are presented in Fig. 13. Moreover, desorption results by various sulfuric and nitric acid concentrations are illustrated in Fig. 14. As these figures show, the best zinc desorption efficiency was 96.6% for 0.1 M H_2SO_4 after 6 h.

Moreover, an adsorption test was performed by the regenerated carbon at the optimum condition, which showed a good result (74% adsorption efficiency with respect to 96.7% adsorption efficiency of the fresh activated carbon).

4. Conclusion

In this work, adsorption of zinc ion from water by activated carbon was investigated. Parameter optimization was performed by experimental design RSM method. The effects of initial metal concentration, pH, and carbon/liquid ratio on

removal efficiency were determined. The initial metal concentration effect was small, while the effects of increasing pH and carbon/liquid ratio were considerable. The optimum zinc removal efficiency was predicted 98.39% at pH = 5.75, adsorbent concentration: 2.5 g of activated carbon in 100 mL solution, and 59.95 mg/L initial concentration. The resulted experimental value at this condition was 96.7%, which showed a good agreement with the predicted value.

Also, kinetic and equilibrium models for zinc removal system were presented. The best kinetic model for Zn removal was determined as pseudo-second-order equation. In the equilibrium study, Temkin and Langmuir equations were well fitted for zinc removal system. In Langmuir equation, the maximum determined adsorption capacity was q_m = 6.53 mg/g.

Then, the co-adsorption removal of Zn and Ni binary mixture ions from water by activated carbon was considered. In this section, Zn removal percentages were enhanced surprisingly in the binary mixture versus single zinc solution. However, a real groundwater may be a multi-component system, and the present work can be continued for such real systems, by considering a specific groundwater analysis, in further studies.

Finally, PRB tests were performed for treatment of single zinc and mixed Zn and Ni solution streams. The lifetime of a constructed PRB for treating zinc-polluted water was determined from the breakthrough curve as 60 h. Also, various regeneration tests for the spent adsorbents were accomplished successfully. The best zinc desorption efficiency was 96.6%, after sulfuric acid washing.

Therefore, the importance of this work is a comprehensive study on the zinc ion adsorption by coal-based activated carbon consisting of kinetics, equilibrium, thermodynamics, RSM optimization of parameters, co-adsorption of Zn and Ni ions, PRB continuous experiments, and regeneration of spent carbon.

References

[1] J.A.B. Mandal, Removal of Cr(VI) from aqueous solution using Bael fruit (*Aegle marmelos correa*) shell as an adsorbent, J. Hazard. Mater., 168 (2009) 633–640.

[2] H. Kalvathy, B. Karthik, L.R. Miranda, Removal and recovery of Ni and Zn from aqueous solution using activated carbon from *Hevea brasiliensis*: batch and column studies, Colloids Surf., B, 78 (2010) 291–302.

[3] Y.F. Lam, L.Y. Lee, S.J. Chua, S.S. Lim, S. Gan, Insights into the equilibrium, kinetic and thermodynamics of nickel removal by environmental friendly *Lansium domesticum* peel biosorbent, Ecotoxicol. Environ. Saf., 127 (2016) 61–70.

[4] F. Fu, Q. Wang, Removal of heavy metal ions from wastewaters: a review, J. Environ. Manage., 92 (2011) 407–418.

[5] A.K. Bhattacharya, S.N. Mandal, S.K. Das, Adsorption of Zn from aqueous solution by using different adsorbents, Chem. Eng. J., 123 (2006) 43–51.

[6] M.N. Siddiqui, H.H. Redhwi, A.A. AlSaadi, M. Rajeh, T.A. Saleh, Kinetic and computational evaluation of activated carbon produced from rubber tires toward the adsorption of nickel in aqueous solutions, Desal. Wat. Treat., 57 (2016) 17570–17578.

[7] D. Mohan, K.P. Singh, Single- and multi-component adsorption of cadmium and zinc using activated carbon derived from bagasse—an agricultural waste, Water Res., 36 (2002) 2304–2318.

[8] G. Wang, A. Li, M. Li, Sorption of nickel ions from aqueous solutions using activated carbon derived from walnut shell waste, Desal. Wat. Treat., 16 (2010) 282–289.

[9] U. Kouakou, A.S. Ello, J.A. Yapo, A. Trokourey, Adsorption of iron and zinc on commercial activated carbon, J. Environ. Chem. Ecotoxicol., 5 (2013) 168–171.

[10] H. Marsh, F.R. Reinoso, Activated Carbon, Elsevier Science and Technology Books, London, 2006.

[11] C. Kirbiyik, A.E. Putun, E. Putun, Comparative studies on adsorptive removal of heavy metal ions by biosorbent, biochar, and activated carbon obtained from low cost agro-residue, Water Sci. Technol., 73 (2016) 423–436.

[12] J. Lach, E. Okoniewska, L. Stępniak, A. Ociepa-Kubicka, The influence of modification of activated carbon on adsorption of Ni(II) and Cd(II), Desal. Wat. Treat., 52 (2014) 3979–3986.

[13] P.C. Mishra, R.K. Patel, Removal of lead and zinc ions from water by low cost adsorbents, J. Hazard. Mater., 168 (2009) 319–325.

[14] G. Jin, Y. Eom, T.G. Lee, Removal of Hg from aquatic environments using activated carbon impregnated with humic acid, J. Ind. Eng. Chem., 42 (2016) 46–52.

[15] N. Esfandiar, B. Nasernejad, T. Ebadi, Removal of Mn from groundwater by sugarcane bagasse and activated carbon (a comparative study): application of response surface methodology (RSM), J. Ind. Eng. Chem. Res., 20 (2014) 3726–3736.

[16] W. Daoud, T. Ebadi, A. Fahimifar, Regeneration of acid-modified activated carbon used for removal of toxic metal hexavalent chromium from aqueous solution by electro kinetic process, Desal. Wat. Treat., 57 (2016) 7009–7020.

[17] P.G. Gonzalez, Y.B. Pliego-Cuervo, Adsorption of Cd(II), Hg(II) and Zn(II) from aqueous solution using mesoporous activated carbon produced from *Bambusa vulgaris striata*, Chem. Eng. Res. Des., 92 (2014) 2715–2724.

[18] O.S. Amuda, A.A. Giwa, I.A. Bello, Removal of heavy metal from industrial wastewater using modified activated coconut shell carbon, Biochem. Eng. J., 36 (2007) 174–181.

[19] B. Saha, M.H. Tai, M. Streat, Metal sorption performance of an activated carbon after oxidation and subsequent treatment, Process Saf. Environ. Prot., 79 (2001) 345–351.

[20] S.A. Haladu, A.M. Muhammad, T.A. Saleh, S.A. Ali, Synthesis of novel cross-linked cyclopolymer bearing polyzwitterion-dianionic moieties and its sorption efficiency for Ni(II) removal from waters, Chem. Eng. Res. Des., 106 (2016) 337–346.

[21] L. Gonsalvesh, S.P. Marinov, G. Gryglewicz, R. Carleer, J. Yperman, Preparation, characterization and application of polystyrene based activated carbons for Ni removal from aqueous solution, Fuel Process. Technol., 149 (2016) 75–85.

[22] A. Damaj, G.M. Ayoub, M. Al-Hindi, H. El Rassy, Activated carbon prepared from crushed pine needles used for the removal of Ni and Cd, Desal. Wat. Treat., 53 (2015) 3371–3380.

[23] M. Ugurlu, I. Kula, M.H. Karaoglu, Y. Arslan, Removal of Ni ions from aqueous solutions using activated carbon prepared from olive stone by $ZnCl_2$ activation, Environ. Prog. Sustain. Energy, 28 (2009) 547–557.

[24] M. Machida, M. Aikawa, H. Tatsumoto, Prediction of simultaneous adsorption of Cu and Pb onto activated carbon by conventional Langmuir type equations, J. Hazard. Mater., 120 (2005) 271–275.

[25] B. Channarong, S.H. Lee, R. Bade, O.V. Shipin, Simultaneous removal of nickel and zinc from aqueous solution by micellar-enhanced ultrafilteration and activated carbon fiber hybrid process, Desalination, 262 (2010) 221–227.

[26] A.R. Gavaskar, Design and construction techniques for permeable reactive barriers, J. Hazard. Mater., 68 (1999) 41–71.

[27] Y. Liu, H. Mou, L. Chen, Z.A. Mirza, L. Liu, Cr(VI)-contaminated groundwater remediation with simulated permeable reactive barrier (PRB) filled with natural pyrite as reactive material: environmental factors and effectiveness, J. Hazard. Mater., 298 (2015) 83–90.

[28] O. Gibert, T. Rotting, J.L. Cortina, J. de Pablo, C. Ayora, J. Carrera, J. Bolzicco, In-situ remediation of acid mine drainage using a permeable reactive barrier in Aznalcóllar spill (SW Spain), J. Hazard. Mater., 191 (2011) 287–295.

[29] K. Sasaki, D.W. Blowes, C.J. Ptacek, W.D. Gould, Immobilization of Se(VI) in mine drainage by permeable reactive barriers: column performance, Appl. Geochem., 23 (2008) 1012–1022.

[30] T.F. Guerin, S. Horner, T. McGovern, B. Davey, An application of permeable reactive barrier technology to petroleum hydrocarbon contaminated groundwater, Water Res., 36 (2002) 15–24.
[31] S.H. Lee, H.Y. Jo, S.T. Yun, Y.J. Lee, Evaluation of factors affecting performance of a zeolitic rock barrier to remove zinc from water, J. Hazard. Mater., 175 (2010) 224–234.
[32] K. Komnitsas, G. Bartzas, I. Paspaliaris, Efficiency of limestone and red mud barriers: laboratory column studies, Miner. Eng., 17 (2004) 183–194.
[33] K. Komnitsas, G. Bartzas, I. Paspaliaris, Modeling of reaction front progress in fly ash permeable reactive barriers, Environ. Forensics, 7 (2006) 219–231.
[34] K. Komnitsas, G. Bartzas, I. Paspaliaris, Inorganic contaminant fate assessment in zero-valent iron treatment walls, Environ. Forensics, 7 (2006) 207–217.
[35] G. Bartzas, K. Komnitsas, Solid phase studies and geochemical modelling of low-cost permeable reactive barriers, J. Hazard. Mater., 183 (2010) 301–308.
[36] K. Komnitsas, G. Bazdanis, G. Bartzas, E. Sahinkaya, D. Zaharaki, Removal of heavy metals from leachates using organic/inorganic permeable reactive barriers, Desal. Wat. Treat., 51 (2013) 3052–3059.
[37] D.D. Do, Adsorption Analysis: Equilibria and Kinetics, Imperial College Press, London, 1998.
[38] R.M. Ali, H.A. Hamad, M.M. Hussein, G.F. Malash, Potential of using green adsorbent of heavy metal removal from aqueous solutions: adsorption kinetics, isotherm, thermo dynamic, mechanism and economic analysis, Ecol. Eng., 91 (2016) 317–332.
[39] T. Depci, A.R. Kul, Y. Onal, Competitive adsorption of lead and zinc from aqueous solution on activated carbon prepared from Van apple pulp: study in single- and multi-solute systems, Chem. Eng. J., 200–202 (2012) 224–236.
[40] N. Balasubramanian, T. Kojima, C. Srinivasakannan, Arsenic removal through electro coagulation: kinetic and statistical modeling, Chem. Eng. J., 155 (2009) 76–82.
[41] H. Xiyili, S. Cetintas, D. Bingol, Removal of some heavy metals onto mechanically activated fly ash: modeling approach for optimization, isotherms, kinetics and thermodynamics, Process Saf. Environ. Prot., 109 (2017) 288–300.
[42] J.J. Moreno-Barbosa, C. Lopez-Velandia, A. del Pilar Maldonado, L. Giraldo, J.C. Moreno-Pirajan, Removal of lead(II) and zinc(II) ions from aqueous solutions by adsorption onto activated carbon synthesized from watermelon shell and walnut shell, Adsorption, 19 (2013) 675–685.
[43] R.C. Bansal, M. Goyal, Activated Carbon Adsorption, Taylor & Francis, London, 2005.
[44] K. Komnitsas, D. Zaharaki, G. Bartzas, G. Kaliakatsou, A. Kritikaki, Efficiency of pecan shells and sawdust biochar on Pb and Cu adsorption, Desal. Wat. Treat., 57 (2016) 3237–3246.
[45] K. Komnitsas, D. Zaharaki, I. Pyliotis, D. Vamvuka, G. Bartzas, Assessment of pistachio shell biochar quality and its potential for adsorption of heavy metals, Waste Biomass Valorization, 6 (2015) 805–816.
[46] F. Wang, Y. Pan, P. Cai, T. Guo, H. Xiao, Single and binary adsorption of heavy metal ions from aqueous solutions using sugarcane cellulose-based adsorbent, Bioresour. Technol., 241 (2017) 482–490.
[47] B. Tiemeyer, N. Ptaffner, S. Frank, K. Kaiser, S. Fiedler, Pore water velocity and ionic strength effects on DOC release from peat-sand mixtures: results from laboratory and field experiments, Geoderma, 296 (2017) 86–97.
[48] M. Ehtiat, S.J. Mousavi, R. Srinivasan, Groundwater modeling under variable operating conditions using SWAT, MODFLOW and MT3DMS: a catchment scale approach to water resources management, Water Resour. Manage., 32 (2018) 1631–1649.
[49] E. Bozau, S. Haubler, W.V. Berk, Hydrogeochemical modeling of corrosion effects and barite scaling in deep geothermal wells of the North German Basin using PHREEQC and PHAST, Geothermics, 53 (2015) 540–547.